AU Binding Proteins Recruit the Exosome to Degrade ARE-Containing mRNAs

Ching-Yi Chen,[1,8] Roberto Gherzi,[1,5,8] Shao-En Ong,[2]
Edward L. Chan,[3] Reinout Raijmakers,[4]
Ger J. M. Pruijn,[4] Georg Stoecklin,[6]
Christoph Moroni,[6] Matthias Mann,[2]
and Michael Karin[1,7]
[1] Department of Pharmacology
Laboratory of Gene Regulation and
    Signal Transduction
University of California, San Diego
La Jolla, California 92093
[2] Protein Interaction Laboratory
University of Southern Denmark-Odense
DK-5230 Odense M
Denmark
[3] Department of Molecular and Experimental
    Medicine
Scripps Clinic and Research Foundation
La Jolla, California 92037
[4] Department of Biochemistry
University of Nijmegen
P.O. Box 9101
NL-6500HB Nijmegen
The Netherlands
[5] Istituto Nazionale per la Ricerca sul Cancro
Largo R. Benzi, 10
16132 Genova
Italy
[6] Institute of Medical Microbiology
University of Basel
CH-4003 Basel
Switzerland

Summary

Inherently unstable mammalian mRNAs contain AU-rich elements (AREs) within their 3′ untranslated regions. Although found 15 years ago, the mechanism by which AREs dictate rapid mRNA decay is not clear. In yeast, 3′-to-5′ mRNA degradation is mediated by the exosome, a multisubunit particle. We have purified and characterized the human exosome by mass spectrometry and found its composition to be similar to its yeast counterpart. Using a cell-free RNA decay system, we demonstrate that the mammalian exosome is required for rapid degradation of ARE-containing RNAs but not for poly(A) shortening. The mammalian exosome does not recognize ARE-containing RNAs on its own. ARE recognition requires certain ARE binding proteins that can interact with the exosome and recruit it to unstable RNAs, thereby promoting their rapid degradation.

Introduction

Gene expression is controlled at the transcriptional and posttranscriptional levels. An important posttranscriptional control is exerted on mRNA stability, which varies considerably from one mRNA species to another and can be modulated by extracellular stimuli (Ross, 1995; Caponigro and Parker, 1996; Wilusz et al., 2001). The rate of mRNA decay is determined by *cis*-acting elements within the mRNA molecule, which are recognized by *trans*-acting factors that act through ill-defined mechanisms. The most common *cis* element responsible for rapid mRNA decay in mammalian cells is the AU-rich element (ARE), present within 3′ untranslated regions (UTRs) of short-lived cytokine, protooncogene, and growth factor mRNAs (Shaw and Kamen, 1986; Chen and Shyu, 1995; Bakheet et al., 2001). AREs promote deadenylation and subsequent degradation of the mRNA body (Shyu et al., 1991; Xu et al., 1997) and may even stimulate 5′ decapping (Gao et al., 2001). Three ARE binding proteins (AUBPs), AUF1, tristetraprolin (TTP), and HuR, were shown to modulate turnover of ARE-containing mRNAs (ARE-RNAs). AUF1 promotes mRNA decay and is also involved in heat shock-induced stabilization of ARE-RNAs (Zhang et al., 1993; Laroia et al., 1999; Loflin et al., 1999). Mice lacking TTP exhibit decreased TNFα and GM-CSF mRNA turnover (Carballo et al., 1998, 2000). TTP binds to AREs of TNFα and other cytokine mRNAs and promotes their deadenylation and decay (Lai et al., 1999). By contrast, HuR stabilizes ARE-RNAs (Fan and Steitz, 1998; Peng et al., 1998; Ford et al., 1999). However, the mechanisms by which AUBPs modulate ARE-RNA turnover were not elucidated.

Understanding the mechanism(s) that regulate mRNA turnover requires the identification of the enzymatic machinery for mRNA degradation. In *Saccharomyces cerevisiae*, two mRNA decay pathways exist (Tucker and Parker, 2000). Both pathways initially involve shortening of the poly(A) tail. Subsequently, the mRNA is degraded in either 5′-to-3′ or 3′-to-5′ directions. In 5′-to-3′ decay, which is the major mRNA degradation pathway in yeast, removal of the cap structure by the Dcp1p decapping enzyme occurs after poly(A) shortening (LaGrandeur and Parker, 1998). Following decapping, the transcript is rapidly degraded by the Xrn1p 5′-to-3′ exonuclease (Hsu and Stevens, 1993). The minor 3′-to-5′ decay pathway depends on a complex of exonucleases, termed the exosome (Mitchell et al., 1997). The yeast exosome, present in both the nucleus and cytoplasm, is composed of at least ten subunits, all of which are 3′-to-5′ exoribonucleases and/or RNA binding proteins (Mitchell et al., 1997; Allmang et al., 1999b; van Hoof and Parker, 1999; Mitchell and Tollervey, 2000). The nuclear exosome, which includes an additional component Rrp6p, is involved in processing of small nuclear and nucleolar RNAs, ribosomal RNAs, and degradation of pre-rRNA spacers and unspliced pre-mRNAs (Mitchell et al., 1997; Allmang et al., 1999a, 2000; Bousquet-Antonelli et al., 2000; van Hoof et al., 2000a). The cytoplasmic exosome participates in mRNA turnover (Jacobs et al., 1998; van Hoof et al., 2000b). The exosome seems to be conserved in higher eukaryotes, where it also appears to be a multiprotein complex (Allmang et al., 1999b; Brouwer et al., 2001). Two putative human exosome components, PM-

[7] Correspondence: karinoffice@ucsd.edu
[8] These authors contributed equally to this work.

Scl100 and PM-Scl75, are part of the PM-Scl particle, a protein complex recognized by autoimmune sera from polymyositis-scleroderma overlap syndrome patients (PM-Scl) (Alderuccio et al., 1991; Ge et al., 1992). To date, eight putative human exosome components were cloned, six of which are found within a multiprotein complex (Allmang et al., 1999b; Brouwer et al., 2001). Two additional human genes, KIAA0116 (accession number D29958) and *OIP-2* (accession number AF025438), are homologous to the yeast *RRP45* gene (Allmang et al., 1999b), but three yeast exosome subunits, Rrp42p, Rrp43p, and Mtr3p, have not been assigned any mammalian homolog. Both yeast and human exosome components display sequence similarity to *E. coli* RNase PH, RNase D, or RNase R (Allmang et al., 1999b; Mitchell and Tollervey, 2000). The roles of the mammalian exosome in mRNA turnover were not defined.

The first step in mammalian mRNA decay also appears to be poly(A) shortening (Shyu et al., 1991). However, the subsequent steps in mammalian mRNA decay are not as well defined as in yeast. It is not even clear whether RNA degradation proceeds via a 5′-to-3′ or 3′-to-5′ pathway. In vitro studies suggest that mammalian mRNA decay occurs via a 3′-to-5′ pathway (Brewer, 1998). However, the enzyme responsible for this pathway was not heretofore identified. Based on sequence similarity between individual yeast and human exosome components, we postulated that the mammalian particle may be functionally homologous to the yeast exosome and therefore responsible for 3′-to-5′ mRNA decay, including rapid turnover of ARE-RNAs. To test this hypothesis, we purified the human exosome, determined its composition, and examined its role in decay of ARE-RNAs using an in vitro mRNA turnover system (Ford et al., 1999) that faithfully replicates the regulation of ARE-directed mRNA degradation (Chen et al., 2000). We show that, indeed, the human exosome contains at least ten subunits and is responsible for exonucleolytic degradation of the RNA body, but is not required for poly(A) shortening. The mammalian exosome is tightly associated with a putative RNA helicase, whose yeast homologs, Ski2p and Mtr4p, have been genetically implicated in mRNA turnover and RNA processing (de la Cruz et al., 1998; Jacobs et al., 1998). Although the purified exosome per se does not exhibit ARE binding activity, it is recruited to ARE-RNAs through interactions with several AUBPs. We demonstrate that AREs function through binding of AUBPs such as KSRP and TTP, which in turn recruit the exosome to affect 3′-to-5′ mRNA degradation.

Results

ARE-RNAs Are Degraded via the Mammalian Exosome

We used a cell-free RNA decay system to investigate the degradation pathway mediated by AREs within cytokine and protooncogene mRNAs. We first examined whether an RNA containing the *c-fos* ARE (ARE^{fos}) was degraded via a 3′-to-5′ pathway, as previously suggested (Brewer, 1998). The RNA was 5′ or 3′ end-labeled, added to a cytosolic extract (S100) of Jurkat cells (Chen et al., 2000), and decay products were analyzed on a denaturing poly-

acrylamide gel (Figure 1A). The 3′-labeled substrate was rapidly degraded and no decay intermediates were observed (Figure 1A, right panel). In contrast, at least one degradation intermediate and a smear of smaller products were observed with the 5′-labeled substrate (Figure 1A, left panel). The smear most likely corresponds to short RNAs, which are not efficiently degraded. These results suggest that the decay is processive with some stalling, as no prominent degradation intermediates could be detected. Although we could not rule out the involvement of other pathways in decay of ARE^{fos} RNA in this system, the detection of decay intermediate only with a 5′ end-labeled substrate suggests the involvement of a 3′-to-5′ pathway (see Discussion).

To investigate whether the mammalian exosome was responsible for degradation of ARE-RNAs in this system, the exosome was removed by sequential immunoprecipitation with autoimmune PM-Scl serum. Immunoblot analysis with antibodies against human exosome components including PM-Scl75, hRrp4p, hRrp40p, hRrp41p, and hRrp46p suggested that the PM-Scl serum removed these exosome subunits (Figure 1B). Capped, either adenylated (Figure 1C, lanes 1–8) or nonadenylated (Figure 1C, lanes 9–16), and uniformly ^{32}P-labeled RNAs, including two ARE-RNAs, IL-2 3′UTR and *c-fos* ARE, and two non-ARE-RNAs, a fragment of GAPDH and a non-ARE random sequence (E4), were produced in vitro and their stability examined in depleted and mock-depleted extracts. As reported (Brewer, 1998; Ford et al., 1999), deadenylation preceded decay of the RNA body in the mock-depleted extract (Figure 1C, lanes 1–4). The presence of an ARE promoted degradation of the RNA body, but little degradation occurred with non-ARE-RNAs. However, partial degradation of E4 RNA was seen after a 3 hr incubation (data not shown). Importantly, the ribonucleases responsible for degradation of ARE-RNAs appear not to require a poly(A) tract, and the ARE-facilitated turnover of the RNA body is independent of the ARE location, which can be very close to the 3′ end, as in ARE^{fos}, or 200 nts away from it, as in IL-2 3′UTR.

Most importantly, whereas IL-2 3′UTR and ARE^{fos} RNAs were rapidly degraded in the mock-depleted extract, they were relatively stable in the PM-Scl-depleted extract (Figure 1C, lanes 5–8 and 13–16). The immunodepletion also prevented partial degradation of E4 RNA seen after prolonged incubation (data not shown). Interestingly, accumulation of prominent decay intermediates of adenylated ARE-RNAs identical in size to the nonadenylated ARE-RNAs was observed in the immunodepleted extract but not in the mock-depleted extract (Figure 1C, lanes 5–8 versus lanes 1–4). Furthermore, deadenylation of non-ARE-RNAs was not impaired by exosome removal, while deadenylation of ARE-RNAs was only slightly retarded. To verify that the decay intermediates represent deadenylated products, polyadenylated IL-2 3′UTR RNA was incubated with mock- or PM-Scl-depleted S100s and the RNA products were isolated and incubated with RNase H in the presence of oligo(dT). This treatment resulted in disappearance of adenylated RNA and appearance of deadenylated products (Figure 1D, lane 7). The smaller of the two RNA species observed after incubation with the depleted extract (Figure 1D, lane 3) was not affected by RNase H treatment and was identical in size to deadenylated RNA (Figure 1D, lane 9).
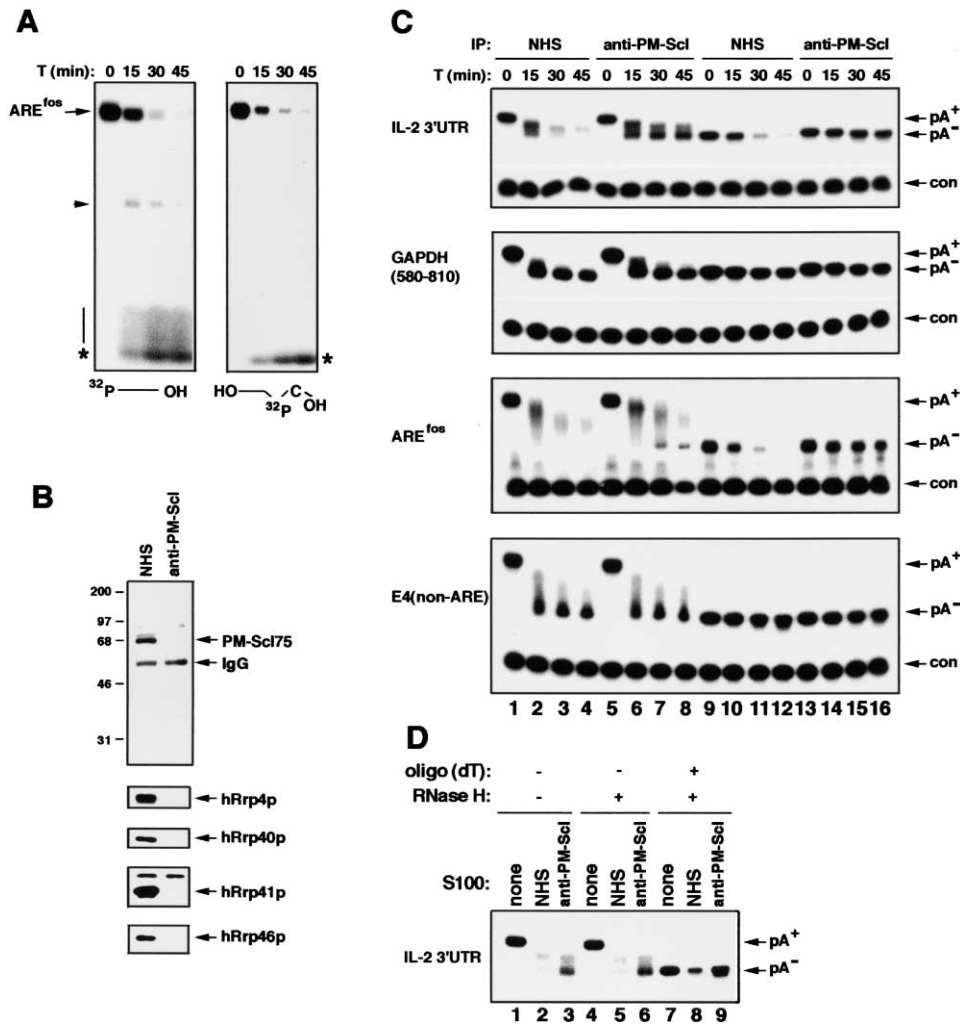
Figure 1. PM-Scl Associated Proteins Are Required for ARE-Mediated RNA Decay

(A) Degradation of an ARE-RNA. ARE[fos] RNA, 5′ or 3′ labeled using T4 polynucleotide kinase and [γ-^{32}P]-ATP or T4 RNA ligase and 5′-[^{32}P]-pCp, respectively, was incubated with Jurkat cell S100. At indicated times, RNA was isolated and analyzed on denaturing polyacrylamide gels. Arrow-intact RNA; arrowhead-decay intermediates. Decay products at the bottom of left panel (indicated by a vertical line) represent inefficiently degraded short RNA fragments. Asterisks-decay products that may be free ribonucleotides.

(B) Immunoblot analysis of S100s depleted with normal human serum (NHS) or anti-PM-Scl serum. Proteins were probed with antibodies to human exosome components as indicated.

(C) RNA decay in exosome-depleted S100. Internally ^{32}P-labeled RNAs (0.5 ng) including ARE-containing 3′ UTR of IL-2 and ARE[fos] or non-ARE-containing GAPDH(580–810) and a short random sequence (E4) were synthesized with (lanes 1–8) or without (lanes 9–16) a 60 nt poly(A) tail. The RNAs were incubated with mock- (NHS) or exosome- (anti-PM-Scl) depleted S100s and their decay analyzed as above. PolyA$^+$ and polyA$^-$ RNAs are indicated. The lower bands marked "con" is external RNA added to the completed reactions to control for recovery and loading.

(D) Decay intermediates observed in exosome-depleted S100 represent deadenylated RNAs. Polyadenylated IL-2 3′UTR RNA was incubated with mock- or exosome-depleted S100s for 45 min, isolated, and further analyzed by RNase H digestion in the absence or presence of oligo(dT).

That form is deadenylated RNA, and it can be concluded that the exosome is not required for deadenylation in this system but is necessary for degradation of deadenylated ARE-RNA bodies.

To exclude that the stabilizing effect of anti-PM-Scl is due to removal of proteins other than the exosome complex, S100s were immunodepleted with antibodies raised to the exosome components hRrp40p and hRrp46p (Brouwer et al., 2001). As this study was focused on the exosome's role in decay of the mRNA body, we used in these and subsequent experiments uniformly labeled nonadenylated RNA substrates. Either antiserum completely removed both hRrp40p and hRrp46p (Figures 2A and 2B) and caused ARE-RNA stabilization (Figure 2C). As a control, anti-hRrp46p was incubated with His-tagged hRrp46p prior to immunodepletion. Immunoblot analysis showed that His-hRrp46p blocked depletion of both hRrp40p and hRrp46p (Figures 2A and 2B). However, a considerable amount of His-hRrp46 was present in the resulting supernatant (Figure 2B). Importantly, preincubation of anti-hRrp46p with His-hRrp46p prevented the stabilization of ARE[fos]
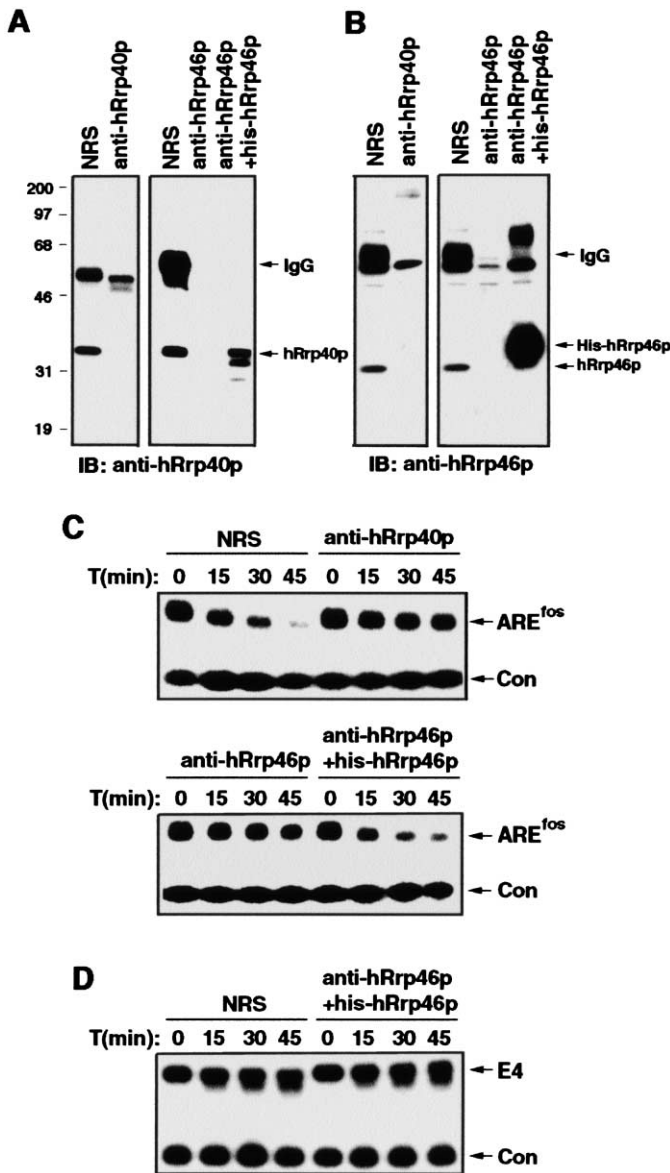
Figure 2. The Exosome Is Required for Rapid Degradation of ARE^fos RNA

(A and B) S100s were depleted by incubation (four times) with protein A-agarose beads loaded with either normal rabbit serum (NRS), anti-hRrp40p, or anti-hRrp46p, or anti-hRrp46p plus His-tagged hRrp46p. The depleted S100s were fractionated and immunoblotted (IB) with anti-hRrp40p (A) or anti-hRrp46p (B) antibodies. (C and D) The stability of ARE^fos (C) or E4 (D) RNAs was examined in the immunodepleted S100s.

RNA (Figure 2C). No effect on stability of E4 RNA was observed (Figure 2D).

Purification of the Human Exosome and Molecular Identification of Its Components

Several components of the PM-Scl particle, including PM-Scl100 and PM-Scl75, are similar to yeast exosome subunits (Allmang et al., 1999b). To biochemically analyze the mammalian exosome, it was purified from Jurkat cell extracts using the tandem affinity purification (TAP) procedure (Rigaut et al., 1999). We introduced the TAP tag at the C terminus of hRrp4p and stably expressed the fusion protein in Jurkat cells. The complex containing hRrp4p-TAP was similar in size to the endogenous complex, as analyzed by gel filtration chromatography (data not shown). hRrp4p-TAP-associated proteins were isolated from either cytoplasmic or nuclear extracts by two-step affinity purification, concentrated, fractionated by SDS-PAGE, and detected by silver staining (Figure 3A).

This analysis revealed 14 polypeptides ranging in size from 20 to 120 kDa, labeled as p1 to p14, that were not present in control preparations isolated from cells expressing the TAP tag alone. The relative levels of p1 to p14 varied significantly with the more abundant species migrating between 25 and 40 kDa.

The relevant bands were excised from the gel and analyzed by mass spectrometry (Table 1). Several proteins previously believed to be part of the human exosome were identified; p7 is hRrp4p-TAP, whereas p10 and p13 are hRrp40p and hCsl4p (Baker et al., 1998; Brouwer et al., 2001), respectively. Two distinct proteins, hRrp41p and hRrp46p (Brouwer et al., 2001), were present within band p12. Bands p8 and p9 contained previously identified gene products, KIAA0116 (accession number D29958) and OIP-2 (accession number AF025438), respectively. Several peptide sequences were obtained from band p11 using electrospray tandem mass spectrometry (Wilm et al. 1996). One of the peptides and

its tandem mass spectrum are shown (Figure 3C). The sequences of the peptides did not match any previously known protein but were encoded by a segment of human genomic clone AC009060 (Figure 3D). Subsequently, a mouse gene (accession number AK012102) that encodes a highly similar protein (92% identify) was found. The two mammalian proteins exhibit sequence similarity to yeast Mtr3p (Figure 3E). Two polypeptides, p1 and p14, were identified that did not exhibit homology to any yeast exosome components. p1 is a previously identified gene product (KIAA0052, accession number P42285) that exhibits striking similarity to yeast Ski2p and Mtr4p (Dangel et al., 1995). Ski2p and Mtr4p were implicated, based on genetic evidence, in mRNA turnover and RNA processing but were not directly shown to stably associate with the exosome (de la Cruz et al., 1998; Brown et al., 2000). p14 was found to be M-phase phosphoprotein 6 (MPP-6; accession number BC005242). The identity of p2, p3, p4, p5, and p6 could not be established by mass spectrometry, probably due to insufficient amounts of material in these bands. However, bands p2, p3, and p4 contained PM-Scl100-, whereas bands p5 and p6 contained PM-Scl75-immunoreactive material, as determined by immunoblotting (Figure 3B). PM-Scl100 was previously shown to be predominantly localized in the nucleus (Allmang et al., 1999b; Brouwer et al., 2001), and its presence in our cytoplasmic fraction is probably due to leakage of nuclear components. In summary, we identified human homologs for ten of the yeast exosome subunits, except for a human homolog of yeast Dis3p.

The Exosome Promotes Rapid Degradation of ARE-RNAs
We examined whether the human exosome isolated by either the TAP procedure or immunoprecipitation with antibodies could restore RNA decay in exosome-depleted extracts. Cytoplasmic or nuclear exosomes isolated from hRrp4p-TAP-expressing cells, but not control preparations isolated from cells expressing the TAP tag alone (see Figure 3A), reconstituted degradation of ARE^{fos} RNA but did not affect E4 RNA (Figures 4A and 4B, top panel). Similar restoration of ARE-RNA degradation was observed with precipitates of anti-hRrp40p or anti-hRrp46p but not control rabbit serum (Figure 4B, bottom panel). The amounts of exosome used for reconstitution experiments were equivalent to those present in mock-depleted S100 (Figure 4A, lane 1). Next we examined whether isolated exosomes discriminate between ARE- and non-ARE-RNAs in the absence of an S100 extract. Extensive degradation of ARE^{fos} RNA was observed with three different amounts of TAP-isolated exosome (Figure 4C). By contrast, at most 50% degradation of E4 RNA was achieved at the highest exosome input. A similar level of E4 RNA degradation observed only after a 3 hr incubation with nondepleted S100 (data not shown). The purified exosome also exhibited preferential degradation of other ARE-RNAs, including the ARE of TNFα mRNA (wtARE^{tnf}) and IL-2 3′UTR, but did not significantly degrade non-ARE-RNAs, including a mutant version of ARE^{tnf} (mARE^{tnf}) and GAPDH (data not shown). Similarly, ARE^{fos}, but not E4 RNA, was completely degraded upon incubation with anti-hRrp40p or anti-hRrp46p immunoprecipitates (Figure 4D).

Interaction of AUBPs with the Exosome and Their Role in Exosome-Mediated Decay of ARE-RNA
The ability of isolated exosomes to preferentially degrade ARE-RNAs was rather surprising. We therefore examined whether the ARE-directed ribonuclease activity reflects an inherent ability of some exosomal components or whether it is due to small amounts of AUBPs that copurify with the exosome. We first checked for AUBPs by UV crosslinking experiments using ARE^{fos} RNA as a probe. After crosslinking, the products were treated with ribonuclease and immunoprecipitated with antiexosome antibodies. Several AUBPs were detected in the crude extract (Figure 5A, lane 1 indicated as "Input" shows all of the proteins that are labeled by crosslinking to the ARE^{fos} probe) and most of them, with the notable exception of an abundant 34 kDa species, were precipitated by anti-hRrp40p, anti-hRrp46p, or anti-PM-Scl, but not by control sera (Figure 5A). As none of these proteins seemed to be an exosome subunit, we examined whether they correspond to known AUBPs. In the course of identifying proteins that interact with the 3′ UTR of IL-2 mRNA, we purified a 78 kDa RNA binding protein and identified it as KSRP, a K-type RNA binding protein (Min et al., 1997; C.-Y.C. and R.G., unpublished results). The 78 kDa AUBP was specifically precipitated by anti-KSRP antibodies (Figure 5B), whereas the 40 kDa and 34 kDa AUBPs were precipitated by antibodies to AUF1 and HuR, respectively (Figure 5B). These data suggest that KSRP and AUF1, but not HuR, may interact with the exosome. Immunoblotting analysis confirmed this conclusion, in which AUF1 and KSRP, but not HuR, were found in exosome preparations purified from cells expressing hRrp4p-TAP (Figure 5C). The interaction between the exosome and KSRP or AUF1 was further confirmed by coprecipitation experiments using RNase-treated extracts. KSRP and AUF1 coprecipitated with the exosome components regardless of RNase treatment (Figure 5D). It should be noted, however, that a considerably higher fraction of KSRP was exosome associated than AUF1. Two other RNA binding proteins, La and nucleolin, were not precipitated (Figure 5D). These results indicate that the observed interactions are specific and RNA independent. Similar results were obtained by gel permeation chromatography (data not shown). To investigate the interaction between the exosome and TTP, also an AUBP, 293 cells were transiently transfected with a vector expressing epitope-tagged TTP. Immunoblotting analysis indicated that TTP was precipitated by anti-PM-Scl but not by control sera (Figure 5E). Among the AUBPs that interact with the exosome, KSRP was not previously known as such. We examined whether recombinant KSRP specifically recognizes an ARE-RNA in UV crosslinking assays. KSRP bound ARE^{fos}, but not E4 RNA, in a concentration-dependent manner (Figure 5F). The binding of KSRP to ARE^{fos} RNA was efficiently competed by unlabeled ARE^{fos} but not E4 RNA (Figure 5G).

We next investigated whether any of these proteins is responsible for targeting the exosome to ARE-RNAs. AUBPs were removed from the S100 by incubation with poly(U)-agarose, as most AUBPs exhibit high affinity to poly(U) RNA (data not shown). Most importantly, AUBPs were effectively removed by this treatment (Figure 6A). Immunoblotting analysis confirmed that KSRP, AUF1,

A

NE   CE

TAP   hRrp4p   TAP   hRrp4p

200 —
116 —
97 —

66 —

45 —

31 —

15 —

p1=KIAA0052
p2
p3] PM-Scl100
p4
p5] PM-Scl75
p6

p7=hRrp4p-TAP
p8=KIAA0116
p9=OIP-2
p10=hRrp40p
p11=hMtr3p
p12=hRrp41p
&hRrp46p
p13=hCsl4p
p14=MPP-6

B

hRrp4p NE   hRrp4p CE   hRrp4p NE   hRrp4p CE

] PM-Scl100

] PM-Scl75

C

LYPVLQQSLVR
m/z 658.39
(2+)

Relative Intensity (%)

55

0

R V   L S   Q   Q   L   V   P   Y L

200   400   600   800   1000

m/z

E

```
hMtr3p:  MP-GDHRRIRGPEESQPPQLYAADEEEAPGTRDPTRL
mMtr3p:  MP-GDHRRIRGPEESQPPQLYAAEDDETPAARDPTRL
yMtr3p:  MNVQDRRRLLGPAAAKP-MAFSNTTTHVPEKKS-TDL
            *  *  ** **   *            *      *

hMtr3p:  RP--------VYARAGLLSQAKGSAYLEAGG----TK
mMtr3p:  RP--------VYARAGLLSQAKGSAYLEAGG----TK
yMtr3p:  TPKGNESEQELSLHTGFIENCNGSALVEARSLGHQTS
            *      *   *** **     *

hMtr3p:  VLCAVSGPRQAEGGERGGGPAGAGGEAPAALRGRLLC
mMtr3p:  VLCAVSGPRQAEGGERGTGPAGAGGEAPAALRGRLLC
yMtr3p:  LITAVYGPRSIRGSFTSQGTISI------QLKNGLLE
           ** ***   *       *          *  **

hMtr3p:  DFRRAPFAGRRRRAPP-GGCEERELALALQEALEPAV
mMtr3p:  DFSRAPFSGRRRRAPQGGGGGEDRELGLALQEALEPAV
yMtr3p:  KYNTN---------------ELKEVSSFLMGIFNSVV
           *       *           *      *      *

hMtr3p:  RLGRYPRAQLEVSALLLEDG------------------
mMtr3p:  RLGRYPRAQLEVSALLLEDG------------------
yMtr3p:  NLSRYPKSGIDIFVYLTYDKDLTNNPQDDDSQSKMMS
           * ***          * *

hMtr3p:  ---GSALAAALTAAALALADAGVEMYDLVVGCGLSLA
mMtr3p:  ---GCALAAALTAAALALADAGVEMYDLVVGCGLSLT
yMtr3p:  SQISSLIPHCITSITLALADAGIE-------------
                      *  *******  *

hMtr3p:  PGPAPTWLLDPTRLEEERAAAGLTVALMPVLNQVAGL
mMtr3p:  PGPSPTWLLDPTRLEEEHSAAGLTVALMPVLNQVAGL
yMtr3p:  -------LVDMAGAGE---ANGTVVSFIKNGEEIVGF
              *  *       *  * * *          *

hMtr3p:  LGSGEGGLTESWAEAVRLGLEGCQRLYPVLQQSLVRA
mMtr3p:  LGSGEGGQTESWTDAVRLGLEGCQRLYPVLQQCLVRA
yMtr3p:  WK--DDGDDEDLLEC----LDRCKEQYNRYRDLMISC
            *             *   *   *

hMtr3p:  ARRRGAAAQP
mMtr3p:  ARRRGAAAPP
yMtr3p:  LMNQET----
```

D

```
    ATGCCTGGGGATCACCGCCGCATCCGCGGCCCTGAAGAA
1   M  P  G  D  H  R  R  I  R  G  P  E  E
    TCGCAGCCGCCGCAGCTGTACGCGGCCGACGAGGAGGAG
14  S  Q  P  P  Q  L  Y  A  A  D  E  E  E
    GCGCCCGGCACCCGCGACCCAACGCGGCTACGGCCCGTG
27  A  P  G  T  R  D  P  T  R  L  R  P  V
    TACGCGCGCGCCGGGCTGCTGAGCCAGGCCAAGGGCTCG
40  Y  A  R  A  G  L  L  S  Q  A  K  G  S
    GCCTACCTGGAGGCGGGAGGCACCAAGGTGCTGTGTGCC
53  A  Y  L  E  A  G  G  T  K  V  L  C  A
    GTGTCGGGCCCGCGACAGGCCGAGGGCGAGCGCGGC
66  V  S  G  P  R  Q  A  E  G  G  E  R  G
    GGCGGGCCCGGCCGGAGCAGGCGGCGAGGCCCCGGCCGCG
79  G  G  P  A  G  A  G  G  E  A  P  A  A
    CTGCGCGGTCGCCTGCTCTGCGACTTCCGCCGCGCACCC
92  L  R  G  R  L  L  C  D  F  R  R  A  P
    TTCGCGGGCCGCCGGCGCCGCGCTCCCCCGGGCGGCTGC
105 F  A  G  R  R  R  R  A  P  P  G  G  C
    GAGGAGCGTGAGCTGGCGCTGGCGCTGCAGGAGGCGCTG
118 E  E  R  E  L  A  L  A  L  Q  E  A  L
    GAGCCGGCTGTGCGCCTGGGCCGCTACCCGCGCGCGCAG
131 E  P  A  V  R  L  G  R  Y  P  R  A  Q
    CTCGAGGTGTCGGCGCTGCTGCTGGAGGACGGTGGCTCG
144 L  E  V  S  A  L  L  L  E  D  G  G  S
    GCCCTGGCCGCCGCGCTCACCGCCGCCGGCGTCGCCCTG
157 A  L  A  A  A  L  T  A  A  A  L  A  L
    GCCGACGCGGGCGTGGAGATGTACGACCTGGTGGTGGGC
170 A  D  A  G  V  E  M  Y  D  L  V  V  G
    TGCGGCCTCAGCCTCGCGCCGGGGCCCGCGCCCACCTGG
183 C  G  L  S  L  A  P  G  P  A  P  T  W
    CTCCTGGACCCCACGCGGCTCGAGGAAGAGCGCGCCGCC
196 L  L  D  P  T  R  L  E  E  E  R  A  A
    GCCGGCCTCACCGTGGCGCTCATGCCTGTGCTGAATCAG
209 A  G  L  T  V  A  L  M  P  V  L  N  Q
    GTGGCCGGGGCTGCTGGGCAGCGGCGAGGGCGGCCTGACA
222 V  A  G  L  L  G  S  G  E  G  G  L  T
    GAGAGCTGGGCGGAGGCCGTACGCCTGGGCCTCGAGGGC
235 E  S  W  A  E  A  V  R  L  G  L  E  G
    TGCCAGCGCCTCTACCCCGTGCTGCAGCAGAGCCTGGTG
248 C  Q  R  L  Y  P  V  L  Q  Q  S  L  V
    CGGGCCGCCCGCCGCAGGGGCGCCGCCGCCCAGCCCTGA
261 R  A  A  R  R  R  G  A  A  A  Q  P  *
```
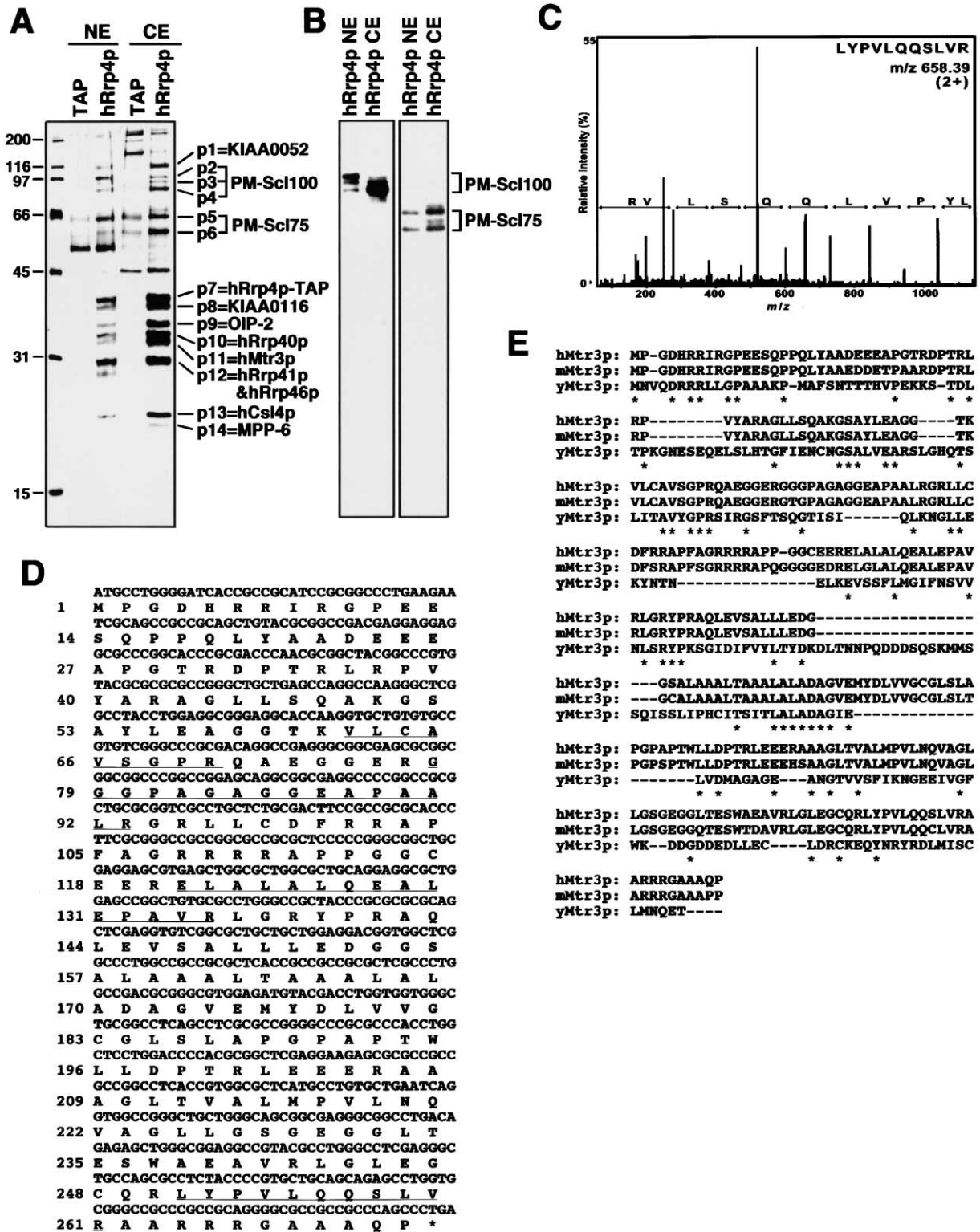
Figure 3. Purification and Composition of the Human Exosome

(A) Cytoplasmic (CE) or nuclear (NE) control and exosome fractions isolated from cells expressing TAP fragment only (TAP) or TAP-tagged hRrp4p (hRrp4p) were fractionated by SDS-PAGE and silver stained. Proteins identified by MALDI and/or nanoelectrospray tandem mass spectrometry are indicated on the right.

(B) Purified nuclear or cytoplasmic exosome preparations were immunoblotted with polyclonal antibodies to PM-Scl100 (left panel) or PM-Scl75 (right panel).

Table 1. Identification of Human Exosome Components

Protein	Peptide Sequence	Match	Yeast Homolog
Core Components			
p7	YIGEVGDIVVGR	hRrp4p	Rrp4p
	LDSVLLLSSMNLPGGELR		43% (52%)
	NCIISLVTQR		
p8	LSVENVPCIVTLCK	hRrp42p	Rrp42p
	GGDDLGTEIANTLYR	(KIAA0116)	25% (51%)
	GSLDPESIFEMMETGKR		
p9	TTTVNIGSISTADGSALVK	hRrp43p	Rrp43p
	AEFAAPSTDAPDK	(OIP-2)	23% (37%)
p10	MAEPASVAAESLAGSR	hRrp40p	Rrp40p
	GDHVIGIVTAK		30% (46%)
	VVCGPGLR		
p11	GGGPAGAGGEAPAALR	hMtr3p	Mtr3p
	ELALALQEALEPAVR	(AC009060)	19% (36%)
	LYPVLQQSLVR		
	VLCAVSGPR		
p12	QTFEAAILTQLHPR	hRrp41p	Rrp41p
	MAGLELLSDQGYR		35% (54%)
	ATLEVILRPK	hRrp46p	Rrp46p
	AVLTFALDSVER		26% (42%)
p13	VHILYVGSMPLK	hCsl4p	Cls4p
	SSENGALPVVSVVR		48% (56%)
	HGYIFSSLAGCLMK		
Associated Factors			
p1	GIVILMVDEK	KIAA0052	Ski2p 34% (51%)
	LTEQLAGPLR		Mtr4p 55% (73%)
p14	IISEEHWYLDLPELK	MPP-6	
	YETLVGTIGK		

Peptide sequences obtained by nano electrospray tandem mass spectrometry are shown. For the yeast homologs, values represent percentage identity (similarity). Values for Rrp4p, Rrp40p, Rrp41p, Rrp46p, and Csl4p are adapted from Allmang et al. (1999b) and Brouwer et al. (2001).

and HuR were completely removed (data not shown), whereas some AUBPs were not depleted (Figure 6A). In contrast to AUBPs, no significant depletion of exosome components was observed (Figure 6B). Thus, although the AUBPs interact with the exosome, they are not tightly associated with it. Alternatively, only a small fraction of the exosome associates with AUBPs. Most importantly, ARE[fos] RNA was much more stable in the poly(U)-depleted S100 than in the poly(G)-depleted S100 (Figures 6C and 6D). Therefore, AUBPs are required for degradation of ARE-RNAs.

Recombinant AUBPs were added to the poly(U)-treated S100 and their effect on ARE-directed RNA decay was examined. While no significant degradation of ARE[fos] RNA was observed upon addition of HuR or AUF1, addition of KSRP or TTP reconstituted degradation of ARE[fos] but had no effect on E4 RNA (Figures 6C and 6D). Similarly, addition of KSRP or TTP, but not AUF1, to the poly(U)-depleted S100 restored degradation of wtARE[tnf] and IL-2 3′UTR RNAs but had no effect on mARE[tnf] and GAPDH RNAs (Figure 6E). To further examine the role of KSRP and TTP in ARE-directed RNA decay, we performed similar experiments using isolated exosomes. By increasing the RNA input (six times more than the amount used in Figure 4C), no significant decay of ARE[fos]

was detected (Figure 6F), suggesting that the amount of AUBPs copurifying with the exosome is indeed low. Addition of recombinant KSRP or TTP to the isolated exosome specifically stimulated the degradation of ARE[fos], although higher inputs of either protein were less effective (Figure 6F). These data strongly suggest that KSRP and TTP are involved in decay of ARE-RNA, probably through their ability to recruit the exosome to the RNA.

Discussion

The rate of mRNA degradation is controlled via *cis*-acting elements within the mRNA molecule (Ross, 1995). The major cis-element responsible for rapid turnover of inherently unstable mammalian mRNAs is the ARE (Shaw and Kamen, 1986; Chen and Shyu, 1995). The mechanism by which the ARE acts remains elusive. Using a cell-free RNA decay system and purified components, we show that AREs recruit the mammalian exosome, a 3′-to-5′ exonuclease, to affect rapid mRNA degradation. This function requires recognition of AREs by AUBPs, several of which are shown to interact with the exosome. To establish the mechanism of ARE-promoted mRNA decay, we first examined which pathway mediates decay of adenylated and deadenylated ARE-RNA in the

(C) Nanoelectrospray tandem mass spectrum of a doubly charged peptide extracted from band p11. Sequence tag was assembled from a series of fragment ions and used to search for a matching pattern.
(D) Nucleotide and predicted amino acid sequences of *hMTR3*. Peptide sequences identified by mass spectrometry are underlined.
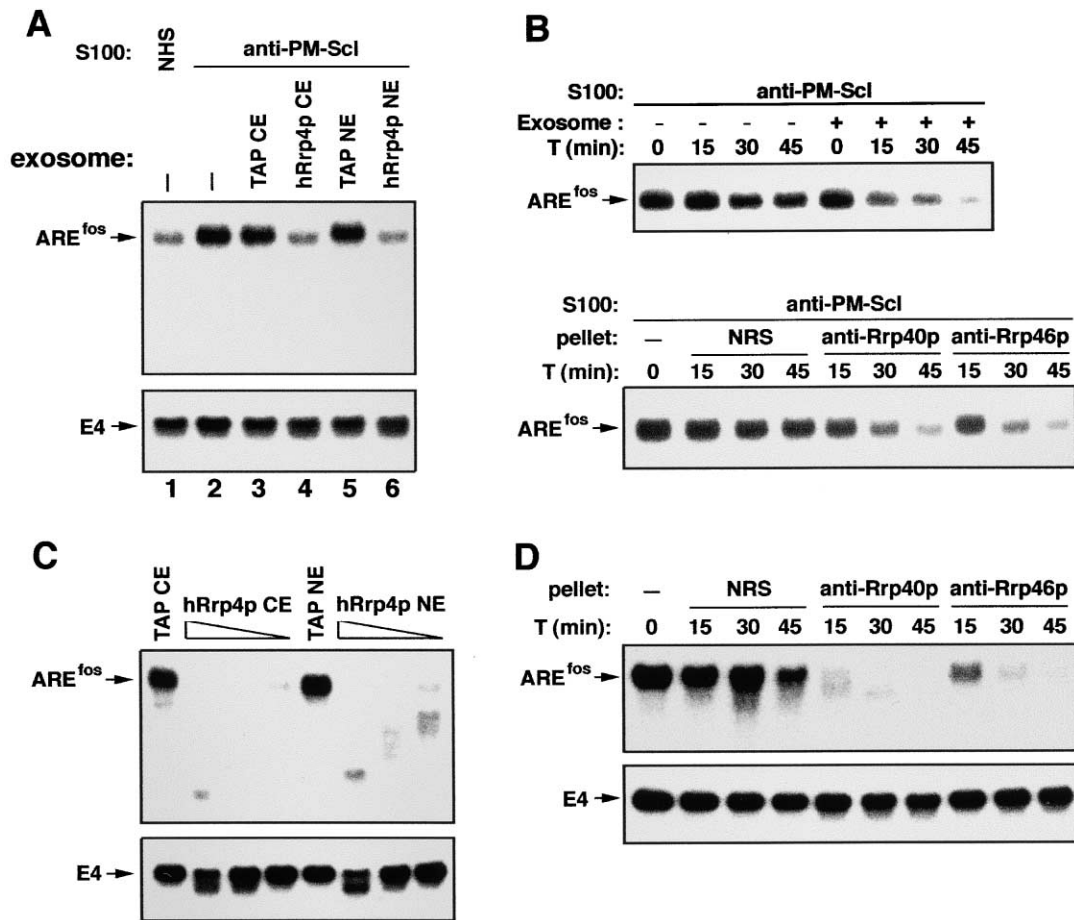(E) Amino acid sequence alignment of mammalian and yeast Mtr3p.

Figure 4. The Purified Exosome Promotes Degradation of ARE-RNA

(A) Reconstitution of ARE-RNA decay in exosome-depleted S100s. Mock-depleted (lane 1, NHS) or anti-PM-Scl-depleted (lanes 2–6, anti-PM-Scl) S100s were supplemented or not (lane 2) with either cytoplasmic (lane 4) or nuclear (lane 6) exosomes or control preparations isolated from cytoplasmic (lane 3) or nuclear (lane 5) extracts of cells that express TAP tag only. ^{32}P-labeled ARE^{fos} or E4 RNAs were added and incubated for 45 min. The levels of remaining RNA were determined.

(B) Isolated exosomes reconstitute ARE^{fos} degradation. Cytoplasmic exosomes (top panel) used in (A) or precipitates of normal rabbit serum (NRS), anti-hRrp40p, or anti-hRrp46p (bottom panel) were added to exosome-depleted S100 and RNA decay assays were performed. The amounts of added exosome components were equivalent to those present in mock-depleted S100.

(C) The purified exosome supports rapid ARE^{fos} decay. ARE^{fos} or E4 RNAs (1 ng) were incubated with 2.5, 5, or 10 μl of purified cytoplasmic (CE) or nuclear (NE) exosomes or control fractions isolated from cytoplasmic and nuclear extracts of cells expressing TAP fragment only. RNA decay was assayed in the presence of 10 mM Na$_2$HPO$_4$. Ten microliters of purified exosome fraction are equivalent to 50% of the amount present in 15 μg of S100.

(D) Immunopurified exosome supports ARE^{fos} degradation. ^{32}P-labeled ARE^{fos} or E4 RNAs were incubated with NRS, anti-hRrp40p, or anti-hRrp46p immunoprecipitates in the presence of 10 mM Na$_2$HPO$_4$ and their decay was examined.

cell-free system (Figure 1A). Although we could not directly demonstrate that ARE-RNAs are degraded via a 3′-to-5′ pathway, immunodepletion of the exosome resulted in almost complete stabilization of ARE-RNAs (Figures 1C and 2C). Given the 3′-to-5′ exonuclease activity of the exosome, these results strongly suggest that the 3′-to-5′ decay pathway is responsible for rapid degradation of ARE-RNAs in our system. Interestingly, removal of the exosome did not substantially interfere with deadenylation. These results are consistent with the role of the cytoplasmic exosome in mRNA turnover in yeast (Jacobs et al., 1998; van Hoof et al., 2000b). Although AREs promote deadenylation in vivo (Shyu et al., 1991; Xu et al., 1997), we did not observe such an effect in our system (Figure 1C). Using HeLa cell extracts

and substrates with long poly(A) tails (200 nts), AREs were reported to slightly enhance deadenylation in vitro (Ford et al., 1999). However, using RNAs with shorter poly(A) tails (60 nts), the same authors could not detect a reproducible effect of the ARE on deadenylation. The lack of strong ARE-facilitated deadenylation in vitro may be due to titration of poly(A) binding protein (PABP) by the large amount of poly(A) RNA added to the reactions, which renders the poly(A) tail freely accessible to deadenylating enzymes. This suggests that ARE-enhanced deadenylation may involve binding of PABP to the poly(A) tail (see below). Regardless of these complications, the present results indicate that the exosome is required for rapid ARE-directed RNA decay. We also found that the exosome is required for decay of non-ARE-RNAs,
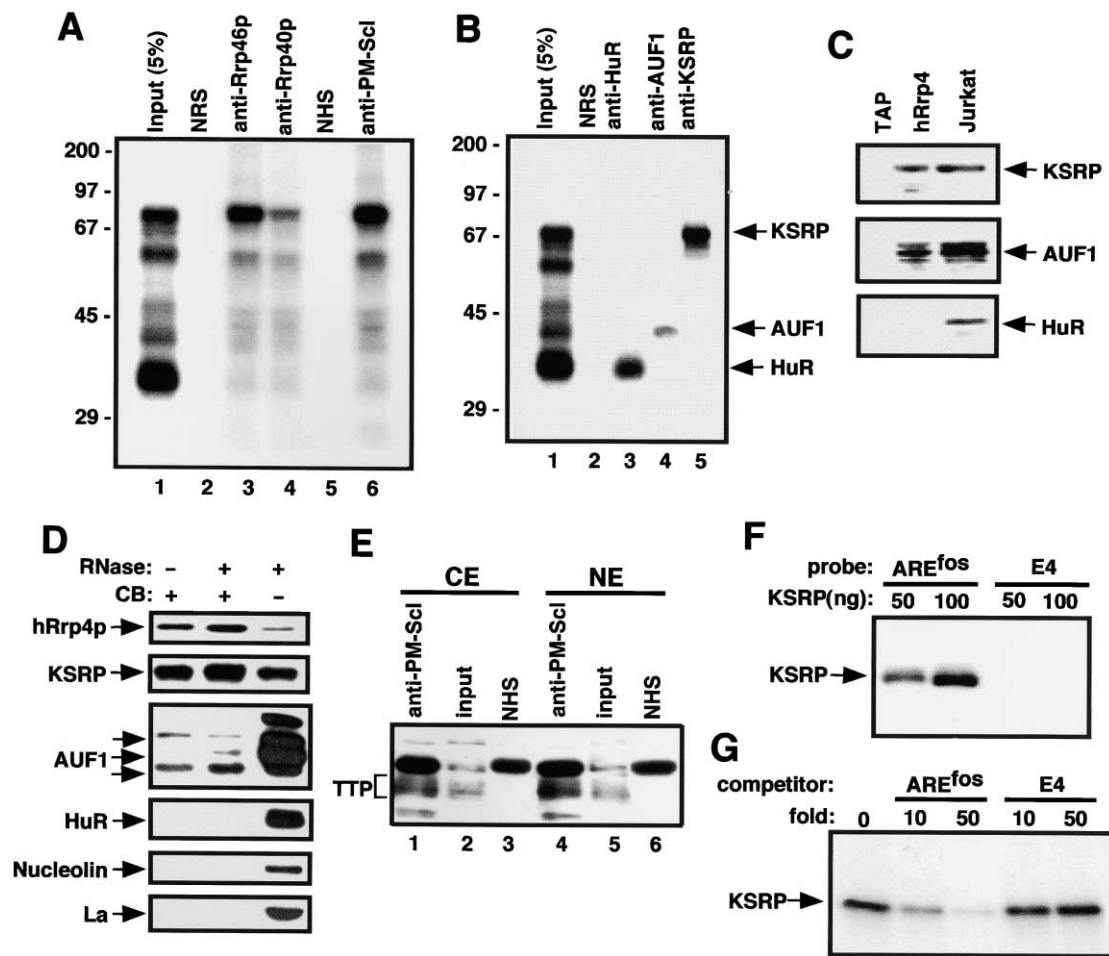
Figure 5. Physical Interactions between AUBPs and the Exosome

(A) Coimmunoprecipitation of AUBPs with the exosome. Jurkat cytoplasmic extracts were incubated with ^{32}P-labeled ARE^{fos} RNA and UV crosslinked. Proteins were immunoprecipitated with NRS, NHS, anti-hRrp46p, anti-hRrp40p, or anti-PM-Scl, separated by SDS-PAGE and autoradiographed. Five percent of the total UV crosslinked extract was loaded onto lane 1.

(B) Identification of AUBPs that bind ARE^{fos} RNA. Proteins crosslinked to ARE^{fos} RNA were immunoprecipitated with antibodies to KSRP, HuR, or AUF1 and analyzed as described in (A).

(C) KSRP and AUF1, but not HuR, copurify with the exosome. Proteins purified by TAP procedure from either control (TAP) or hRrp4p-TAP-expressing cells were immunoblotted with antibodies to KSRP, AUF1, or HuR. Total Jurkat cytoplasmic extract was loaded onto lane 3.

(D) Cytoplasmic extracts of hRrp4p-TAP-expressing cells were either untreated (lane 1) or treated (lane 2) with RNase A (0.5 mg/ml) for 30 min at 37°C. hRrp4p-TAP and associated proteins were precipitated with calmodulin beads (CB) or not and analyzed as indicated. Five percent of nonprecipitated extracts were loaded onto lane 3.

(E) TTP coprecipitates with the exosome. Cytoplasmic or nuclear extracts of 293 cells transiently expressing myc-TTP were immunoprecipitated with NHS or anti-PM-Scl and analyzed by immunoblotting with anti-myc antibody. Ten percent of the unprecipitated input were loaded onto lanes 2 and 5.

(F) KSRP binds ARE^{fos} RNA. Recombinant KSRP (50 or 100 ng) was incubated with either ^{32}P-labeled ARE^{fos} or E4 RNA probes, and UV crosslinking assays were performed.

(G) Specific binding of KSRP to ARE^{fos} RNA. KSRP (100 ng) was incubated with ^{32}P-labeled ARE^{fos} RNA in the presence of different amounts (10- or 50-fold excess) of cold ARE^{fos} or E4 RNAs and analyzed by UV crosslinking.

which is rather inefficient and requires prolonged incubation (data not shown).

By incorporating a tagged hRrp4p into the human exosome, we were able to purify it and determine its composition by mass spectrometry. The human exosome is similar in structure to its yeast counterpart, containing at least ten subunits. With the exception of hDis3p, we identified human homologs of all yeast exosome subunits. Two proteins, previously known as KIAA0116 and OIP-2, were identified as the human homologs of Rrp42p and Rrp43p, respectively. Another

newly identified human exosome component is likely to be the homolog of Mtr3p. All three of these human proteins exhibit similarity to E. coli RNase PH and are therefore likely to be bona fide exosome subunits. The relative paucity of high-molecular weight subunits in the purified exosome (Figure 3A) could be due to their proteolysis during isolation, as we found several bands recognized by antibodies to each PM-Scl antigen (Figure 3B). We also identified at least two exosome-associated proteins. One of which, encoded by the KIAA0052 open reading frame, is homologous to yeast Ski2p and
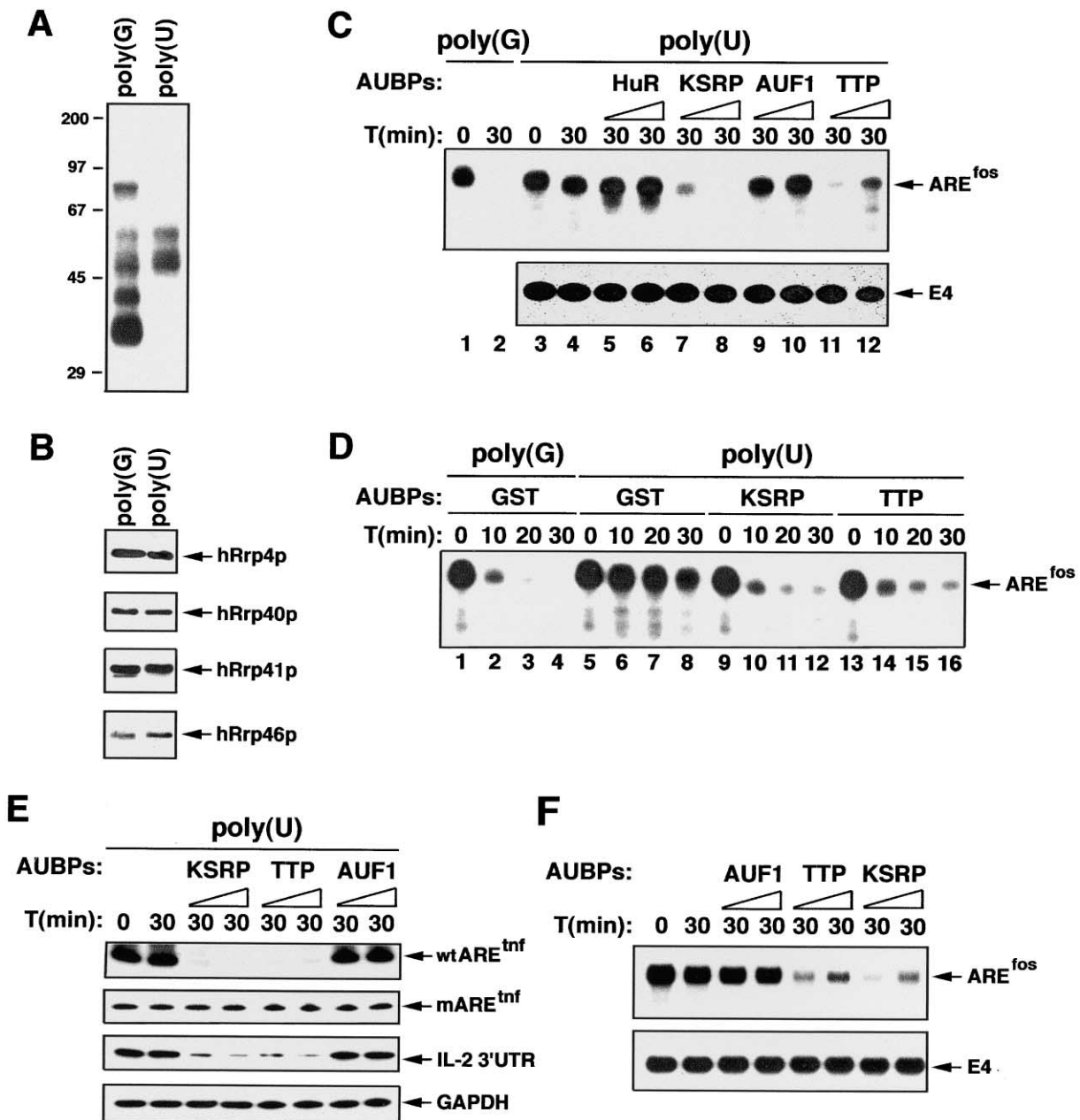
Figure 6. AUBPs Are Required for Exosome-Mediated ARE-RNA Decay

(A) Depletion of AUBPs by poly(U)-agarose. Jurkat S100s were incubated with either poly(G)- or poly(U)-agarose beads. Supernatants were examined by UV crosslinking assays using ^{32}P-labeled ARE^{fos} RNA.

(B) Exosome components are not removed by either poly(G)- or poly(U)-agarose. Poly(G)- or poly(U)-depleted supernatants were analyzed by immunoblotting with antibodies to exosome components.

(C) Degradation of ARE^{fos} RNA is AUBP dependent. ^{32}P-labeled ARE^{fos} or E4 RNAs were incubated with poly(G)- (lanes 1 and 2) or poly(U)- (lanes 3–12) depleted S100s supplemented or not with 25 or 100 ng of recombinant AUBPs, as indicated. Levels of remaining RNA were examined.

(D) KSRP and TTP restore degradation of ARE^{fos} RNA. ^{32}P-labeled ARE^{fos} RNA was incubated with poly(G)- or poly(U)-depleted S100s in the presence of GST (100 ng), KSRP (100 ng), or GST-TTP (25 ng) and its decay was examined.

(E) KSRP and TTP stimulate degradation of ARE- but not of non-ARE-RNAs. ^{32}P-labeled wtARE^{tnf}, mARE^{tnf}, IL-2 3′UTR, or GAPDH RNAs were incubated with poly(U)-depleted S100 supplemented or not with 25 or 100 ng of recombinant AUBPs, as indicated. Levels of remaining RNA were examined.

(F) KSRP or TTP stimulate degradation of ARE^{fos} by the exosome. ^{32}P-labeled ARE^{fos} or E4 RNAs (6 ng) were incubated with purified cytoplasmic exosome in the absence or presence of AUF1, TTP, or KSRP (12.5 or 25 ng) and levels of remaining RNA were examined.

Mtr4p that are believed to interact with the exosome and provide it with RNA helicase activity. The other protein, MPP-6, was previously identified as a protein phosphorylated during mitosis. The functional relationships of these proteins to the mammalian exosome remain to be explored.

The purified exosome restored rapid degradation of ARE-RNAs when added to exosome-depleted extracts. Similar activity was exhibited by purified cytoplasmic and nuclear exosomes in the absence of other added components. The ability of the exosome to discriminate between ARE-RNAs and non-ARE-RNAs was unanticipated, and indeed, additional experiments have shown that discrimination depends on the presence of AUBPs, several of which copurify with the exosome. The presence of AUBPs in purified exosome preparations was demonstrated by UV crosslinking and immunoblotting experiments. However, it should be noted that no AUBP could be identified as an abundant exosome-associated protein by mass spectrometry. Indeed, immunoprecipitation experiments have revealed the association of the exosome with only a fraction of the total pool of KSRP and even a small portion of total AUF1. However, the small amounts of associated AUBPs are functional and account for the exosome ability to preferentially target ARE-RNAs. Indeed, depletion of AUBPs with poly(U) beads prevented preferential degradation of ARE-RNAs by the exosome. Furthermore, the use of higher amounts of RNA substrates in the decay experiments, which is likely to titrate residual AUBPs, resulted in stabilization of ARE-RNAs. Under these conditions, addition of at least two recombinant AUBPs, KSRP and TTP, to purified exosome preparations restored the preferential and rapid degradation of ARE-RNAs. Interestingly, the effect of either KSRP or TTP on exosome-mediated degradation of certain ARE-RNAs was biphasic. Most likely, small amounts of either protein suffice for effective recruitment of the exosome to ARE-RNA, but higher amounts may prevent such recruitment through titration of AUBP binding sites on both the exosome and the RNA substrate.

KSRP was originally identified as a component of protein complex assembled on an intronic *c-src* enhancer required for neuronal-specific splicing (Min et al., 1997). We found that KSRP is also an exosome-interacting AUBP capable of promoting ARE-mediated decay, at least in vitro. The other protein shown to have such an activity, TTP, is well established as a stimulator of ARE-mediated mRNA turnover in vivo (Lai et al., 1999; Stoecklin et al., 2000; Ming et al., 2001). Both KSRP and TTP do not stimulate degradation of substrates lacking functional AREs. Surprisingly, recombinant AUF1 did not enhance ARE-mediated mRNA decay in the reconstituted system, although it was reported to do so in vivo (Loflin et al., 1999). However, we cannot exclude the possibility that the recombinant form of AUF1, although having ARE binding activity (data not shown), was not properly folded or posttranslationally modified. The structural basis for the interaction of AUBPs with the exosome has not been determined. These interactions, although RNA independent, could be direct or indirect and may be mediated by a specific exosome targeting sequence motif. Needless to say, this is an important topic for further investigation. At least one AUBP, HuR, was shown to promote RNA stabilization rather than decay (Fan and Steitz, 1998; Peng et al., 1998; Ford et al., 1999). No HuR could be detected in purified exosome preparation (Figures 5C and 5D, and unpublished data). Thus, the stabilizing activity of HuR may be due to its inability to recruit the exosome to ARE-RNAs.

Whether the exsome is involved in 3′-to-5′ decay of ARE-RNA in vivo awaits further investigation, but preliminary results suggest that partial inhibition of exosome subunit synthesis using antisense RNA results in stabilization of ARE-RNA in living cells (unpublished data). Most importantly, the cell-free decay system used in the present study has proven to be invaluable for investigating the mechanistic aspects of mammalian mRNA turnover. Despite a few discrepancies, this system is able to reproduce several aspects of mRNA turnover observed in vivo, such as ARE-facilitated mRNA decay and decapping, as well as signal-induced mRNA stabilization (Ford, et al., 1999; Chen et al., 2000; Gao, et al., 2000, 2001). Although the mechanism by which AUBPs promote decay of ARE-RNAs deserves further investigation, we can propose a simple working model that is consistent with currently available results. Binding of some AUBPs to AREs may alter the interactions between PABP and the poly(A) tail or between cap binding proteins and the 5′ cap, thereby providing access to the poly(A) ribonuclease (PARN) and the decapping enzyme (Gao et al., 2000, 2001; Wilusz et al., 2001). Alternatively, AUBPs may recruit PARN and the decapping enzyme to the RNA substrate. At the same time, AUBPs, such as TTP and KSRP, recruit the exosome to the vicinity of ARE-RNAs to initiate degradation of the RNA body after deadenylation is completed. Alternatively, AUBPs recruit a large, but loosely assembled, degradative machinery containing PARN, the decapping enzyme, and the exosome. This recruitment-based mechanism explains why ARE-RNAs are preferentially degraded and why they are stabilized upon ARE removal. The present results also suggest that AUBPs may be important targets for some of the signaling pathways by which extracellular stimuli stabilize ARE-RNAs.

Similar to yeast, decay of mammalian mRNAs is initiated via deadenylation (Shyu et al., 1991). Unlike yeast, in which both 5′-to-3′ and 3′-to-5′ decay pathways exist (Tucker and Parker, 2000), the subsequent steps of mammalian mRNA turnover have not been elucidated in vivo. We show that the exosome is responsible for 3′-to-5′ decay of ARE-RNAs in vitro. If they can be extrapolated to intact cells, these results suggest that the 3′-to-5′ pathway may be the predominant decay pathway of ARE-RNAs. As recent results suggest that ARE-mediated mRNA decay may exist in yeast (Vasudevan and Peltz, 2001), it is important to identify AUBPs in this organism and determine their potential involvement, as well as that of the exosome, in this phenomenon. The availability of a biochemical system based on purified components and genetic studies in yeast should facilitate the analysis of AUBP function and determination of the molecular basis for both stabilizing and destabilizing activities.

Experimental Procedures

Plasmids
DNAs used to produce RNA substrates were subcloned into pCY2, a derivative of pSP64poly(A) (Promega), in which a linker [5′-GGTAC

CCTCGAG(AAAAAA)₁₀GAATTC-3'] was inserted between the *SacI* and *EcoRI* sites. DNA fragments containing the 3' UTR of IL-2 (590–780 nt) or GAPDH (580–810 nt) were subcloned between the *HincII* and *KpnI* or *HindIII* and *XbaI* sites of pCY2, respectively. ARE^fos and E4 were constructed by inserting linkers containing the ARE of *c-fos* mRNA (Xu et al., 1997) and a non-ARE sequence (5'-TTATGTT GAATGTTAAATATAGTATCTATGTAGATTGGTTAGTAAAACT-3') between the *HindIII* and *SacI* sites, and *PstI* and *XbaI* sites of pCY2, respectively. Linkers containing the ARE of TNFα mRNA, 5'-ATTAT TTATTATTTATTTATTATTTATTTATTTAATATT-3, or its mutant version, in which the underlined TT dinucleotides were changed to GG, were subcloned between the *HindIII* and *XhoI* sites of pCY2. DNA fragment encoding calmodulin binding peptide, TEV protease recognition sequences, and two IgG binding units of protein A was PCR amplified from pBS1479 (from B. Seraphin at EMBL-Heidelberg) and subcloned between the *XhoI* and *XbaI* sites of pcDNA3 to obtain pcDNA3-TAP, into which a PCR fragment containing the coding region of hRRP4 was subcloned inframe between the *EcoRV* and *XhoI* sites. The myc-tagged TTP vector was described (Stoecklin et al., 2000). Construction of plasmids expressing GST-AUF1 and GST-TTP will be described elsewhere (X.-F Ming and C. Moroni, personal communication). pBac-KSRP was constructed by subcloning *EcoRI-NotI* fragment, lacking the first 46 amino acids of human KSRP (Min et al., 1997), into the same sites of pAcHLTA (Pharmingen).

Preparation of Substrates and In Vitro RNA Decay and UV Crosslinking Analysis

Plasmids were linearized with *EcoRI* or *XhoI* and used to produce internally ³²P-labeled RNA substrates (Chen et al., 2000). When *EcoRI*-linearized plasmids were used, RNAs containing a poly(A) tail of 60 residues followed by a G were obtained. *XhoI*-linearized plasmids yield identical RNAs lacking a poly(A) tail. For 5' or 3' end labeling, unlabeled RNA was prepared, and following alkaline phosphatase treatment, was labeled as described (Caruccio and Ross, 1994) and gel purified. In vitro analysis of RNA decay and S100 preparation from Jurkat cells were described (Chen et al., 2000). Typically, ³²P-labeled RNA (0.5 ng) was incubated with S100 (15 μg) in 25 μl buffer containing 100 mM KCH₃COOH, 2 mM Mg(CH₃COOH)₂, 10 mM Tris (pH 7.6), 2 mM DTT, 10 mM creatine phosphate, 1 μg creatine phosphokinase, 1 mM ATP, 0.4 mM GTP, and 0.1 mM spermine. UV crosslinking was performed by incubating extract (10–20 μg) and ³²P-labeled RNA in a 20 μl RNA binding buffer (Chen et al., 2000) at room temperature for 20 min; 100 U of RNase T1 were added, the samples incubated at 37°C for 15 min, followed by UV irradiation, treatment with RNase A (200 μg per reaction), and SDS-PAGE separation or immunoprecipitation.

Immunodepletion Experiments

The exosome was removed from Jurkat S100 by four 2-hr rounds of immunoprecipitation at 4°C with antisera prebound to Protein A-Sepharose. Equal amounts of supernatants from normal serum- and antiserum-depleted reactions were analyzed by immunoblotting and subsequently used in RNA decay assays. Precipitates were washed and used for reconstitution and RNA decay analysis. AUBPs were depleted by incubating (3 rounds of 2h at 4°C) extracts with poly(U)- or poly(G)-agarose beads (Sigma).

Protein Purification and Sequence Determination

Jurkat cells were transfected with pcDNA3-hRRP4-TAP and stable transfectants were selected and pooled. hRrp4p-TAP and associated proteins were purified using the TAP procedure (Rigaut et al., 1999). Cytoplasmic extracts were prepared by lysing frozen cells at 4°C in lysis buffer (10 mM HEPES [pH 7.6] 3 mM MgCl₂, 10 mM KCl, 5% glycerol, 0.5% NP-40, and 10 μg/ml of aprotinin and leupeptin, 1 mM PMSF). Nuclei were removed by centrifugation, washed twice with lysis buffer, and extracted with lysis buffer containing 400 mM KCl. After centrifugation, KCl concentration of supernatants was adjusted to 100 mM. Cytoplasmic and nuclear extracts were subjected to two-step affinity purification. After 2 hr incubation with IgG Sepharose (200 μl) at 4°C, the beads were washed three times with IPP150 (10 mM Tris [pH 8.0], 150 mM NaCl, and 0.1% NP-40), once with TEV buffer (IPP150 containing 0.5 mM EDTA and 1mM DTT), and incubated in 1 ml TEV buffer containing 100 U of TEV protease

(GIBCO) at room temperature for 2 hr. Supernatants were diluted to 4 ml with calmodulin binding buffer (10 mM β-mercaptoethanol, 10 mM Tris-Cl [pH 8.0], 150 mM NaCl, 1 mM Mg-acetate, 1 mM imidazole, 2 mM CaCl₂, and 0.1% NP40), 100 μl of calmodulin beads (Stratagene) were added, and incubated at 4°C for 2 hr. After washing, bound proteins were eluted (five times, 200 μl each) with calmodulin elution buffer (10 mM β-mercaptoethanol, 10 mM Tris-Cl [pH 8.0], 150 mM NaCl, 1 mM Mg-acetate, 1 mM imidazole, and 2 mM EGTA, 0.1% NP40).

The 78 kDa RNA binding protein (p78) was purified using established procedures (Chen et al., 2000). Jurkat cytoplasmic extract (250 mg protein) was loaded on a 5 ml HiTrap SP column. After washing, proteins were eluted with 100 ml buffer with a linear 100 mM to 1 M KCl gradient, and p78 was identified by UV crosslinking assay using IL-2 3'UTR RNA as a probe. Fractions containing p78 were pooled and subjected to gel filtration chromatography. Peak p78 fractions were pooled and subjected to RNA affinity chromatography using IL-2 3'UTR as a ligand (Chen et al., 2000).

Purified proteins were concentrated by Centricon YM-10 (Amicon) and analyzed by SDS-PAGE, followed by silver staining. Protein bands were excised and subjected to in-gel reduction, alkylation, and tryptic digestion. Digests were desalted and concentrated on a microcolumn packed into GELoader tips (Wilm and Mann, 1996). Peptides were eluted with 1 μl 50% methanol in 5% formic acid directly into a nanospray needle and the eluate subjected to MS and MS/MS analysis on a QSTAR Pulsar quadrupole time-of-flight tandem mass spectrometer (AB/MDS-Sciex, Toronto, Canada) equipped with a nanoelectrospray ion source (MDS Proteomics). Proteins were identified by searching peptide sequence tags, derived from fragment ion spectra of selected peptides, against the nonredundant protein database maintained and updated regularly at the European Bioinformatics Institute (EBI, Hinxton, UK) using the program PepSea (MDS Proteomics).

Recombinant Proteins and Antibodies

GST- and histidine-tagged proteins were produced in BL21(DE3) cells and purified on GSH-Sepharose 4B (Pharmacia Biotech) and Ni-NTA (Qiagen) resins, respectively. Histidine-tagged KSRP was expressed in Sf9 cells and purified by Ni-NTA chromatography. Anti-hRrp4p, anti-hRrp40p, anti-hRrp41p, anti-hRrp46p, and anti-KSRP were described (Min et al., 1997; Mitchell et al., 1997; Brouwer et al., 2001). Autoimmune sera from PM-Scl patients and polyclonal anti-PM-Scl75 antibodies were also described (Alderuccio et al., 1991). Monoclonal antibody to HuR and anti-AUF1 were provided by H. Furneaux and G. Brewer, respectively.

References

Alderuccio, F., Chan, E.K., and Tan, E.M. (1991). Molecular characterization of an autoantigen of PM-Scl in the polymyositis/scleroderma overlap syndrome: a unique and complete human cDNA encoding an apparent 75-kD acidic protein of the nucleolar complex. J. Exp. Med. *173*, 941–952.

Allmang, C., Kufel, J., Chanfreau, G., Mitchell, P., Petfalski, E., and Tollervey, D. (1999a). Functions of the exosome in rRNA, snoRNA and snRNA synthesis. EMBO J. *18*, 5399–5410.

Allmang, C., Petfalski, E., Podtelejnikov, A., Mann, M., Tollervey, D., and Mitchell, P. (1999b). The yeast exosome and human PM-Scl are

related complexes of 3′→5′ exonucleases. Genes Dev. 13, 2148–2158.

Allmang, C., Mitchell, P., Petfalski, E., and Tollervey, D. (2000). Degradation of ribosomal RNA precursors by the exosome. Nucleic Acids Res. 28, 1684–1691.

Baker, R.E., Harris, K., and Zhang, K. (1998). Mutations synthetically lethal with cep1 target S. cerevisiae kinetochore components. Genetics 149, 73–85.

Bakheet, T., Frevel, M., Williams, B.R., Greer, W., and Khabar, K.S. (2001). ARED: human AU-rich element-containing mRNA database reveals an unexpectedly diverse functional repertoire of encoded proteins. Nucleic Acids Res. 29, 246–254.

Bousquet-Antonelli, C., Presutti, C., and Tollervey, D. (2000). Identification of a regulated pathway for nuclear pre-mRNA turnover. Cell 102, 765–775.

Brewer, G. (1998). Characterization of c-myc 3′ to 5′ mRNA decay activities in an in vitro system. J. Biol. Chem. 273, 34770–34774.

Brouwer, R., Allmang, C., Raijmakers, R., van Aarssen, Y., Egberts, W.V., Petfalski, E., van Venrooij, W.J., Tollervey, D., and Pruijn, G.J. (2001). Three novel components of the human exosome. J. Biol. Chem. 276, 6177–6184.

Brown, J.T., Bai, X., and Johnson, A.W. (2000). The yeast antiviral proteins Ski2p, Ski3p, and Ski8p exist as a complex in vivo. RNA 6, 449–457.

Caponigro, G., and Parker, R. (1996). Mechanisms and control of mRNA turnover in Saccharomyces cerevisiae. Microbiol. Rev. 60, 233–249.

Carballo, E., Lai, W.S., and Blackshear, P.J. (1998). Feedback inhibition of macrophage tumor necrosis factor-alpha production by tristetraprolin. Science 281, 1001–1005.

Carballo, E., Lai, W.S., and Blackshear, P.J. (2000). Evidence that tristetraprolin is a physiological regulator of granulocyte-macrophage colony-stimulating factor messenger RNA deadenylation and stability. Blood 95, 1891–1899.

Caruccio, N., and Ross, J. (1994). Purification of a human polyribosome-associated 3′ to 5′ exoribonuclease. J. Biol. Chem. 269, 31814–31821.

Chen, C.Y., and Shyu, A.B. (1995). AU-rich elements: characterization and importance in mRNA degradation. Trends Biochem. Sci. 20, 465–470.

Chen, C.Y., Gherzi, R., Andersen, J.S., Gaietta, G., Jürchott, K., Royer, H.D., Mann, M., and Karin, M. (2000). Nucleolin and YB-1 are required for JNK-mediated interleukin-2 mRNA stabilization during T-cell activation. Genes Dev. 14, 1236–1248.

Dangel, A.W., Shen, L., Mendoza, A.R., Wu, L., and Yu, C.Y. (1995). Human helicase gene SKI2W in the HLA class III region exhibits striking structural similarities to the yeast antiviral gene SKI2 and to the human gene KIAA0052: emergence of a new gene family. Nucleic Acids Res. 23, 2120–2126.

de la Cruz, J., Kressler, D., Tollervey, D., and Linder, P. (1998). Dob1p (Mtr4p) is a putative ATP-dependent RNA helicase required for the 3′ end formation of 5.8S rRNA in Saccharomyces cerevisiae. EMBO J. 17, 1128–1140.

Fan, X.C., and Steitz, J.A. (1998). Overexpression of HuR, a nuclear-cytoplasmic shuttling protein, increases the in vivo stability of ARE-containing mRNAs. EMBO J. 17, 3448–3460.

Ford, L.P., Watson, J., Keene, J.D., and Wilusz, J. (1999). ELAV proteins stabilize deadenylated intermediates in a novel in vitro mRNA deadenylation/degradation system. Genes Dev. 13, 188–201.

Gao, M., Fritz, D.T., Ford, L.P., and Wilusz, J. (2000). Interaction between a poly(A)-specific ribonuclease and the 5′ cap influences mRNA deadenylation rates in vitro. Mol. Cell 5, 479–488.

Gao, M., Wilusz, C.J., Peltz, S.W., and Wilusz, J. (2001). A novel mRNA-decapping activity in HeLa cytoplasmic extracts is regulated by AU-rich elements. EMBO J. 20, 1134–1143.

Ge, Q., Frank, M.B., O'Brien, C., and Targoff, I.N. (1992). Cloning of a complementary DNA coding for the 100-kD antigenic protein of the PM-Scl autoantigen. J. Clin. Invest. 90, 559–570.

Hsu, C.L., and Stevens, A. (1993). Yeast cells lacking 5′→3′ exoribo-

nuclease 1 contain mRNA species that are poly(A) deficient and partially lack the 5′ cap structure. Mol. Cell. Biol. 13, 4826–4835.

Jacobs, J.S., Anderson, A.R., and Parker, R.P. (1998). The 3′ to 5′ degradation of yeast mRNAs is a general mechanism for mRNA turnover that requires the SKI2 DEVH box protein and 3′ to 5′ exonucleases of the exosome complex. EMBO J. 17, 1497–1506.

LaGrandeur, T.E., and Parker, R. (1998). Isolation and characterization of Dcp1p, the yeast mRNA decapping enzyme. EMBO J. 17, 1487–1496.

Lai, W.S., Carballo, E., Strum, J.R., Kennington, E.A., Phillips, R.S., and Blackshear, P.J. (1999). Evidence that tristetraprolin binds to AU-rich elements and promotes the deadenylation and destabilization of tumor necrosis factor alpha mRNA. Mol. Cell. Biol. 19, 4311–4323.

Laroia, G., Cuesta, R., Brewer, G., and Schneider, R.J. (1999). Control of mRNA decay by heat shock-ubiquitin-proteasome pathway. Science 284, 499–502.

Loflin, P., Chen, C.Y., and Shyu, A.B. (1999). Unraveling a cytoplasmic role for hnRNP D in the in vivo mRNA destabilization directed by the AU-rich element. Genes Dev. 13, 1884–1897.

Min, H., Turck, C.W., Nikolic, J.M., and Black, D.L. (1997). A new regulatory protein, KSRP, mediates exon inclusion through an intronic splicing enhancer. Genes Dev. 11, 1023–1036.

Ming, X.-F., Stoecklin, G., Lu, M., Looser, R., and Moroni, C. (2001). Parallel and independent regulation of interleukin-3 mRNA turnover by phosphatidylinositol 3-kinase and p38 mitogen-activated protein kinase. Mol. Cell. Biol., 21, 5778-5789.

Mitchell, P., Petfalski, E., Shevchenko, A., Mann, M., and Tollervey, D. (1997). The exosome: a conserved eukaryotic RNA processing complex containing multiple 3′→5′ exoribonucleases. Cell 91, 457–466.

Mitchell, P., and Tollervey, D. (2000). Musing on the structural organization of the exosome complex. Nat. Struct. Biol. 7, 843–846.

Peng, S.S., Chen, C.Y., Xu, N., and Shyu, A.B. (1998). RNA stabilization by the AU-rich element binding protein, HuR, an ELAV protein. EMBO J. 17, 3461–3470.

Rigaut, G., Shevchenko, A., Rutz, B., Wilm, M., Mann, M., and Séraphin, B. (1999). A generic protein purification method for protein complex characterization and proteome exploration. Nat. Biotechnol. 17, 1030–1032.

Ross, J. (1995). mRNA stability in mammalian cells. Microbiol. Rev. 59, 423–450.

Shaw, G., and Kamen, R. (1986). A conserved AU sequence from the 3′ untranslated region of GM-CSF mRNA mediates selective mRNA degradation. Cell 46, 659–667.

Shyu, A.B., Belasco, J.G., and Greenberg, M.E. (1991). Two distinct destabilizing elements in the c-fos message trigger deadenylation as a first step in rapid mRNA decay. Genes Dev. 5, 221–231.

Stoecklin, G., Ming, X.-F., Losser, R., and Moroni, C. (2000). Somatic mRNA turnover mutants implicate tristetraprolin in the interleukin-3 mRNA degradation pathway. Mol. Cell. Biol. 20, 3753–3763.

Tucker, M., and Parker, R. (2000). Mechanisms and control of mRNA decapping in Saccharomyces cerevisiae. Annu. Rev. Biochem. 69, 571–595.

van Hoof, A., and Parker, R. (1999). The exosome: a proteasome for RNA? Cell 99, 347–350.

van Hoof, A., Lennertz, P., and Parker, R. (2000a). Yeast exosome mutants accumulate 3′-extended polyadenylated forms of U4 small nuclear RNA and small nucleolar RNAs. Mol. Cell. Biol. 20, 441–452.

van Hoof, A., Staples, R.R., Baker, R.E., and Parker, R. (2000b). Function of the ski4p (Csl4p) and Ski7p proteins in 3′-to-5′ degradation of mRNA. Mol. Cell. Biol. 20, 8230–8243.

Vasudevan, S., and Peltz, S.W. (2001). Regulated ARE-mediated mRNA decay in Saccharomyces cerevisiae. Mol. Cell 7, 1191–1200.

Wilm, M., and Mann, M. (1996). Analytical properties of the nanoelectrospray ion source. Anal. Chem. 68, 1–8.

Wilm, M., Shevchenko, A., Houthaeve, T., Breit, S., Schweigerer, L., Fotsis, T., and Mann, M. (1996). Femtomole sequencing of proteins

from polyacrylamide gels by nano-electrospray mass spectrometry. Nature *379*, 466–469.

Wilusz, C.J., Wormington, M., and Peltz, S.W. (2001). The cap-to-tail guide to mRNA turnover. Nat. Rev. Mol. Cell. Biol. *2*, 237–246.

Xu, N., Chen, C.Y., and Shyu, A.B. (1997). Modulation of the fate of cytoplasmic mRNA by AU-rich elements: key sequence features controlling mRNA deadenylation and decay. Mol. Cell. Biol. *17*, 4611–4621.

Zhang, W., Wanger, B.J., Ehrenman, K., Schaefer, A.W., DeMaria, C.T., Crater, D., DeHaven, K., Long, L., and Brewer, G. (1993). Purification, characterization, and cDNA cloning of an AU-rich element RNA-binding protein, AUF1. Mol. Cell. Biol. *13*, 7652–7665.